INTERNATIONAL JOURNAL OF
NUMERICAL ANALYSIS AND MODELING
Volume 12, Number 3, Pages 567–591

AN ADAPTIVE IMMERSED FINITE ELEMENT METHOD WITH ARBITRARY LAGRANGIAN-EULERIAN SCHEME FOR PARABOLIC EQUATIONS IN TIME VARIABLE DOMAINS

ZHIMING CHEN, ZEDONG WU, AND YUANMING XIAO

Abstract. We first propose an adaptive immersed finite element method based on the a posteriori error estimate for solving elliptic equations with non-homogeneous boundary conditions in general Lipschitz domains. The underlying finite element mesh need not fit the boundary of the domain. Optimal a priori error estimate of the proposed immersed finite element method is proved. The immersed finite element method is then used to solve parabolic problems in time variable domains together with an arbitrary Lagrangian-Eulerian (ALE) time discretization scheme. An a posteriori error estimate for the fully discrete immersed finite element method is derived which can be used to adaptively update the time step sizes and finite element meshes at each time step. Numerical experiments are reported to support the theoretical results.

Key words. Immersed finite element, adaptive, a posteriori error estimate, time variable domain.

1. Introduction

Partial differential equations in time variable domains have tremendous interests in scientific and engineering applications including, for example, fluid-structure interaction [4, 18, 16] or melting process [5]. We consider in this paper the following parabolic equations in a time variable domain

$$\frac{\partial u}{\partial t} - \Delta u = f \quad \text{in } \Omega(t),\ \text{a.e. } t \in (0,T), \tag{1}$$

$$u = 0 \quad \text{on } \Gamma(t),\ \text{a.e. } t \in (0,T), \tag{2}$$

$$u = u_0 \quad \text{in } \Omega(0), \tag{3}$$

where $T > 0$ is the length of the time interval, $\Omega(t) \subset \mathbb{R}^2$ is a bounded domain at time t with Lipschitz boundary $\Gamma(t)$. We remark that the results in this paper can be easily extended to deal with problems with non-homogeneous Dirichlet boundary condition and other types of boundary conditions such as Neumann or Robin conditions.

Let $F_t : \hat{\Omega} \to \Omega(t)$ be the bijective map which for any $t \in (0,T)$, maps the reference domain $\hat{\Omega}$ to $\Omega(t)$. The problem (1)-(3) will be discretized in time by the following arbitrary Lagrangian-Eulerian (ALE) scheme [16, 17] (see also section 3 below):

$$\frac{U^n - \bar{U}^{n-1}}{\tau_n} - \mathbf{v}^n \cdot \nabla U^n - \Delta U^n = f^n \quad \text{in } \Omega^n = \Omega(t^n), \tag{4}$$

where $\bar{U}^{n-1}$ and $\mathbf{v}^n$ are defined by

$$\bar{U}^{n-1} = U^{n-1}(F_{t^{n-1}}(F_{t^n}^{-1}(x))), \quad \mathbf{v}^n = (\partial_t F_t)|_{t=t^n}(F_{t^n}^{-1}(x)), \quad \forall x \in \Omega^n.$$

Received by the editors January 10, 2015.
2000 *Mathematics Subject Classification.* 65N15, 65N30.
The first author was supported in part by National Basic Research Project under the grant 2011CB309700 and China NSF under the grant 11021101 and 11321061. The third author was supported in part by the Fundamental Research Funds for the Central Universities under grant 1118020303 and China NSF under the grant 11101208.

One approach is to solve (4) by the finite element method using the mesh which is the map of a fixed finite element mesh in the reference domain $\hat{\Omega}$. This approach has the difficulty of possible mesh distortions which may lead to undesirable remeshing procedures in practical applications. We also remark that the ALE scheme is closely related to the variable mesh method in [20] whose convergence is also studied in [26].

In this paper we propose to solve (4) by using the immersed finite element method in which the finite element meshes need not fit the boundary of the domain. This allows one to combine the technique of adaptive finite element method based on a posteriori error estimates to obtain a fully adaptive algorithm for solving (1)-(3) with error control which achieves quasi-optimal error reduction as solving parabolic equations on time invariant domains (cf. [6]). We remark that immersed finite element or finite difference methods have been extensively studied in the literature. In the finite difference setting, we refer to the immersed boundary method in [28], the immersed interface method in [22, 24], the ghost fluid method in [27], and the references therein. In the finite element framework, we refer to the work of [25, 10] for elliptic problems with discontinuous coefficients in which finite element basis functions are locally modified for elements intersection the interface where the coefficient jumps. In [8] the adaptive immersed interface finite element method based on a posteriori error estimates is proposed for elliptic and Maxwell equations with discontinuous coefficients.

In this paper we first develop an adaptive immersed finite element method based on the a posteriori error estimate for solving elliptic equations with non-homogeneous boundary condition in general Lipschitz domains. We remark that the a posteriori error estimation and adaptive finite element methods for elliptic problems are extensively studied in the literature for polygonal domains with the exception of [12] in which boundary fitted finite element meshes are used. The boundary fitted finite element mesh has the difficulty in refining boundary elements which may destroy the mesh shape regular property if mesh regularization techniques are not used. In this paper we extend the construction of immersed interface finite element in [8] and propose an immersed finite element method to solve elliptic problems on domains with piecewise smooth boundary. Our construction is equivalent to solving the problem on a boundary fitted finite element mesh that satisfies the maximum angle condition. Thus optimal a priori error estimates are guaranteed if the solution are smooth in $H^2(\Omega)$. We also derive a reliable and efficient a posteriori error estimate by introducing a Clément type interpolation operator and using a result of [15] to localize the approximation error of the non-homogeneous boundary condition in $H^{1/2}$ norm. We also refer to the work of [30] and the references therein for the study of a posteriori error estimation for elliptic problems with non-homogeneous boundary conditions in polygonal or polyhedral domains.

We next apply the immersed finite element method for the elliptic problem developed in the first part of this paper to solve the ALE scheme (12) and obtain a fully discrete immersed finite element method for (1)-(3). We derive an a posteriori error estimate of residual type which can be used to adapt the meshes and time step sizes in practical computations. The derived a posteriori error estimate reduces to the standard a posteriori error estimates for parabolic equations in e.g. [29, 7] if the domains are not variable in time. The new difficulty of estimating the parabolic extension of the discrete boundary data on the variable time domain is overcome by using a deep theorem of Verchota in harmonic analysis on the solvability of

Dirichlet problem of Laplace equation with L^p boundary value in general Lipschitz domains.

The layout of the paper is as follows. In section 2 we study the immersed finite element method for the elliptic problem. In section 3 we introduce the ALE scheme and the fully discrete finite element discretization. In section 4 we derive the a posteriori error estimates for the fully discrete method in section 3. In section 5 we report numerical examples to illustrate the competitive performance of the adaptive immersed finite element method based on the a posteriori error estimates derived in this paper.

2. The elliptic problem

Let Ω be a domain in $\mathbb{R}^2$ with the Lipschitz boundary Γ. Given $f \in H^{-1}(\Omega)$, $g \in H^{1/2}(\Gamma)$, we consider in this section the problem to find the solution $u \in H^1(\Omega)$ such that $u = g$ on Γ and

$$\int_\Omega \nabla u \cdot \nabla v \, dx = \langle f, v\rangle_\Omega, \ \forall v \in H_0^1(\Omega), \tag{5}$$

where $\langle \cdot, \cdot\rangle_\Omega$ is the duality pairing between $H^{-1}(\Omega)$ and $H_0^1(\Omega)$. The existence and uniqueness of the above problem is well-known by Lax-Milgram lemma.

2.1. The immersed finite element method.

Let Ω be included in a polygonal domain Ω_h and $\mathcal{M}_h$ be a shape regular mesh over Ω_h. The elements in Ω_h have non-empty intersection with Ω. For the element K that has non-empty intersection with the boundary Γ, we assume Γ intersects the boundary of K at most twice. This assumption is not very restrictive in practical applications if the mesh is sufficiently refined near the boundary. We call the elements that intersect Γ through two sides the type I immersed boundary element and the elements that intersect Γ at one vertex and one interior point of the opposite side the type II immersed boundary element. The other elements that have non-empty intersection with Γ are called non-immersed boundary elements (see Fig. 2.1).

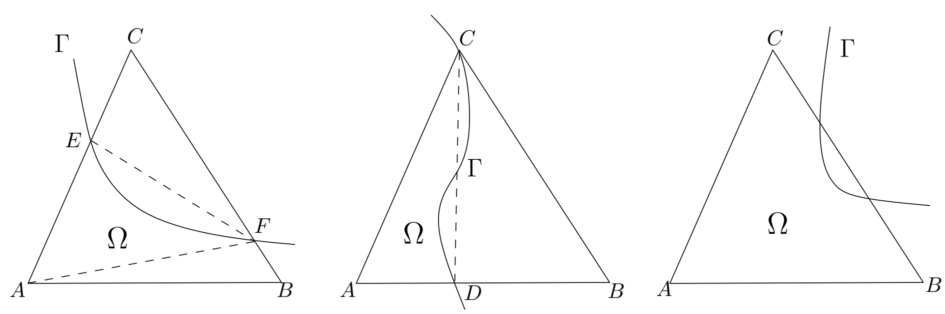

FIGURE 1. The type I immersed boundary element (left), the type II immersed boundary element (middle), and the non-immersed boundary element (right).

For any $K \in \mathcal{M}_h$, we let $V_h(K) = P_1(K)$ for any element K which lies entirely inside Ω or is a non-immersed boundary element. For the type I immersed boundary element K, we connect the two intersection points of Γ which then splits K into a triangle and a quadrilateral. We further break the quadrilateral into two triangles by connecting the diagonal that divides one of the larger inner angle opposite to the two vertices of K (see Fig. 2.1). For the type II immersed boundary element K, it naturally breaks into two triangles by connecting the vertex and the intersection point Γ on the opposite side (see Fig. 2.1).

We define the following immersed finite element space

$$V_h(K) = \{v \in C(K) : v \text{ is linear in each of the sub-triangles of } K\}.$$

The degrees of freedom of functions in $V_h(K)$ are their values at vertices and the intersection points on the sides. We have the following interpolation error estimate.

Lemma 2.1. *Let K be the immersed boundary element. Let $u \in H^2(K)$ and $I_h u$ be its Lagrange interpolant, then we have*

$$\|u - I_h u\|_{L^2(K)} + h_K \|\nabla(u - I_h u)\|_{L^2(K)} \le C h_K \|u\|_{H^2(K)},$$

where h_K is the diameter of the element K.

Proof. We show that the sub-triangles satisfy the maximum angle condition and thus the lemma follows from the well-known interpolation estimates, cf. e.g. [3, 19]. The type II immersed boundary element satisfies trivially the maximum angle condition. For the type I immersed boundary element K as shown in Fig. 2.1, let θ_0 be the minimum angle of K. It is clear that the maximum angles of ΔCEF and ΔABF are bounded above by $\pi - \theta_0$. For the triangle ΔAEF, we first notice that $\angle AEF \ge \theta_0$, thus the angles $\angle FAE$ and $\angle AFE$ are bounded above by $\pi - \theta_0$. Next since $\angle BFE \ge \angle AEF$, we have

$$2\pi = \angle BFE + \angle AEF + \angle CAB + \angle ABC \ge 2\angle AEF + 2\theta_0.$$

This completes the proof. □

Let $V_h(\Omega_h) = \{v \in C(\Omega_h) : v|_K \in V_h(K) \text{ for any } K \in \mathcal{M}_h\}$ be the finite element space over Ω_h and $V_h^0(\Omega_h)$ be the set of all functions in $V_h(\Omega_h)$ that vanish at all degrees of freedom on Γ and the nodes outside Ω. The functions in $V_h^0(\Omega_h)$ are supported in $\tilde{\Omega}_h = \Omega_h \backslash \bar{\Omega}_h^{\text{out}}$, where Ω_h^{out} is the union of all sub-triangles of the immersed boundary elements which have at least one vertex outside $\bar{\Omega}$.

We assume $f \in L^2(\Omega)$ and extend it to be zero outside Ω. Let g_h be some approximation of g defined on $\Gamma_h = \partial\tilde{\Omega}_h$. We define the following finite element approximation of the problem (5): Find $u_h \in V_h(\Omega_h)$ such that $u_h = g_h$ on Γ_h and

$$\int_{\Omega_h} \nabla u_h \cdot \nabla v_h dx = \int_{\Omega_h} f v_h dx, \quad \forall v_h \in V_h^0(\Omega_h). \tag{6}$$

We remark that the problem (6) is equivalent to the conforming linear finite element approximation over $\tilde{\Omega}_h$. We use the formulation in (6) because we find it is convenient for developing the adaptive finite element method. In the following, for the sake of definiteness, we always set u_h to be zero at the nodes outside $\bar{\Omega}$.

The following lemma will be useful for our analysis [23, Lemma 3.4].

Lemma 2.2. *Let D be a bounded domain in $\mathbb{R}^2$ with Lipschitz boundary Γ_D. Let $S_\sigma(\Gamma_D) = \{x \in D : \operatorname{dist}(x, \Gamma_D) < \sigma\}$ be the σ-neighborhood of Γ_D. Then we have*

$$\|u\|_{L^2(S_\sigma(\Gamma_D))} \le C\sqrt{\sigma}\|u\|_{H^1(D)}, \ \forall u \in H^1(D),$$

for some constant C independent of σ.

Theorem 2.3. *Let Γ be C^2 and $u \in H^2(\Omega)$. Let g_h be the Lagrange interpolation of g. Then we have*

$$||\nabla(u - u_h)||_{L^2(\tilde{\Omega}_h)} \le Ch||u||_{H^2(\Omega)},$$

where $h = \max_{K \in \mathcal{M}_h} h_K$.

Proof. By Stein extension theorem [1, Theorem 5.24], we can extend $u \in H^2(\Omega)$ to some $\tilde{u} \in H^2(\mathbb{R}^2)$ such that $\|\tilde{u}\|_{H^2(\mathbb{R}^2)} \le C\|u\|_{H^2(\Omega)}$. Denote $v_h = u_h - I_h\tilde{u} \in V_h^0(\Omega_h)$, where $I_h\tilde{u}$ is the Lagrange interpolation of $\tilde{u}$ in $\tilde{\Omega}_h$ and is zero at the nodes outside $\tilde{\Omega}_h$. Then by (6)

$$\begin{aligned}\|\nabla v_h\|^2_{L^2(\tilde{\Omega}_h)} &= \int_{\tilde{\Omega}_h} f v_h dx - \int_{\tilde{\Omega}_h} \nabla I_h\tilde{u}\cdot\nabla v_h dx\\ &= \int_{\tilde{\Omega}_h} f v_h dx - \int_{\tilde{\Omega}_h} \nabla \tilde{u}\cdot\nabla v_h dx + \int_{\tilde{\Omega}_h} \nabla(\tilde{u} - I_h\tilde{u})\nabla v_h dx,\end{aligned}$$

which, by using integration by parts in the first term and the Cauchy-Schwarz inequality and Lemma 2.1 in the second term, yields

$$\|\nabla v_h\|^2_{L^2(\tilde{\Omega}_h)} \le \int_{\tilde{\Omega}_h} (f + \Delta\tilde{u}) v_h dx + Ch\|\tilde{u}\|_{H^2(\tilde{\Omega}_h)}\|\nabla v_h\|_{L^2(\tilde{\Omega}_h)}.$$

Since $f + \Delta u = 0$ in Ω and the width of $\tilde{\Omega}_h\backslash\bar{\Omega}$ is bounded by Ch^2 because Γ is C^2, we can use Lemma 2.2 to get

$$\int_{\tilde{\Omega}_h} (f + \Delta\tilde{u}) v_h dx \le \|f + \Delta\tilde{u}\|_{L^2(\tilde{\Omega}_h)}\|v_h\|_{\tilde{\Omega}_h\backslash\bar{\Omega}} \le Ch\|f + \Delta\tilde{u}\|_{L^2(\tilde{\Omega}_h)}\|\nabla v_h\|_{\tilde{\Omega}_h}.$$

This implies $\|\nabla v_h\|_{L^2(\tilde{\Omega}_h)} \le Ch\|\tilde{u}\|_{H^2(\tilde{\Omega}_h)} \le Ch\|u\|_{H^2(\Omega)}$. The lemma now follows from the triangle equality and the error estimate in Lemma 2.1. $\square$

2.2. A posteriori error analysis. We start by recalling the Clément interpolation operator on the shape regular mesh [11]. Let $\{x_j\}_{j=1}^{\bar{J}}$ be the set of nodes of the mesh $\mathcal{M}_h$ and denote $\{\psi_j\}_{j=1}^{\bar{J}}$ the corresponding nodal basis function of H^1-conforming linear finite element space over $\mathcal{M}_h$, i.e., $\psi_j(x_i) = \delta_{ij},\ 1 \le i \le \bar{J}$. For any x_j, define $S_j = \mathrm{supp}(\psi_j)$, the star surrounding x_j. The standard Clément interpolant for functions in $L^1(\Omega_h)$ is defined as

$$(\Pi_h\varphi)(x) = \sum_{j=1}^{\bar{J}} (R_j\varphi)(x_j)\psi_j(x),\ \forall\varphi \in L^1(\Omega_h),$$

where $R_j : L^1(S_j) \to P_1(S_j)$ is a local L^2 projection operator, that is, $R_j\varphi \in P_1(S_j)$ such that

$$\int_{S_j} (R_j\varphi) v_h dx = \int_{S_j} \varphi v_h dx,\ \forall v_h \in P_1(S_j).$$

Now we define an interpolation operator $\Pi_h^0 : L^1(\Omega_h) \to V_h^0(\Omega_h)$. Let $\{x_j\}_{j=1}^{J}$ be the set of nodes of $\mathcal{M}_h$ such that S_j is included in Ω (see Fig. 2 where only V_0, V_1 are such nodes). The modified Clément interpolant Π_h^0 is then defined as

$$(\Pi_h^0\varphi)(x) = \sum_{j=1}^{J} (R_j\varphi)(x_j)\psi_j(x),\ \forall\varphi \in L^1(\Omega_h). \tag{7}$$

Notice that $\Pi_h^0\varphi$ vanishes in all boundary elements and thus belongs to $V_h^0(\Omega_h)$.

For any element $K \in \mathcal{M}_h$, if K is included inside Ω or is a non-immersed boundary element, we denote $\mathcal{E}(K)$ the set of the sides of K that are not on $\partial\tilde{\Omega}_h$, and if K is an immersed boundary element, we let $\mathcal{E}(K)$ be the set of all line segments whose end-points are one vertex of K inside Ω and one intersection point of Γ and ∂K. The set of all line segments in $\mathcal{E}(K)$, $K \in \mathcal{M}_h$, is denoted as $\mathcal{B}_h$.

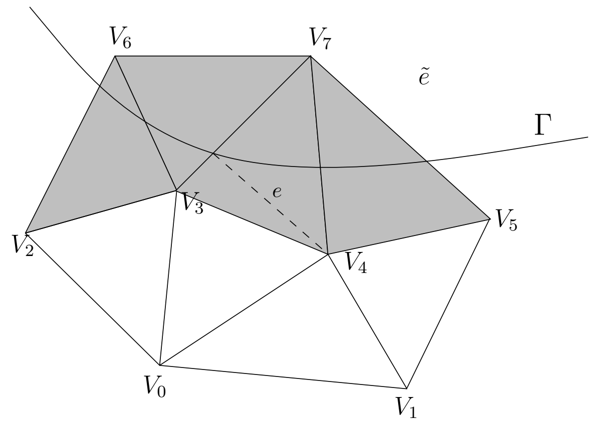

FIGURE 2. A typical boundary element T.

Lemma 2.4. *There exists a constant $C > 0$ depending only on the minimum angle of $\mathcal{M}_h$ such that for any $\varphi \in H_0^1(\Omega)$ which, for convenience, is extended by zero outside Ω if necessary and is still denoted by φ,*

$$\|\varphi - \Pi_h^0 \varphi\|_{L^2(K)} \leq C h_K \|\nabla\varphi\|_{L^2(\tilde{K})}, \ \forall K \in \mathcal{M}_h, \tag{8}$$

$$\|\varphi - \Pi_h^0 \varphi\|_{L^2(e)} \leq C \tilde{h}_e^{1/2} \|\nabla\varphi\|_{L^2(\tilde{e})}, \ \forall e \in \mathcal{E}(K) \text{ not on } \partial\tilde{\Omega}_h, \tag{9}$$

where $\tilde{K}$ is the union of all elements having non-empty intersection with K, $\tilde{h}_e = \min(h_K, h_{e,\Gamma})$ with $h_{e,\Gamma} = \max_{x\in e}\min_{y\in\Gamma}|x-y|$ being the distance between e and Γ, $\tilde{e}$ is a patched of elements surrounding e. Fig. 2 shows a possible configuration for $\tilde{e}$.

Proof. To show (8) we first notice that by the standard error estimates for Clément interpolation operator [11], $\Pi_h\varphi$ satisfies the estimates (8). Thus we only need to consider $\|\Pi_h\varphi - \Pi_h^0\varphi\|_{L^2(K)}$. It is clear that we only need to consider the case when K has one or several nodes x_j whose support of the basis function S_j is not entirely included in Ω. The set of such nodes are denoted $N(K)$. For $x_j \in N(K)$, we have

$$\begin{aligned} |(R_j\varphi)(x_j)| &\leq \left|(R_j\varphi)(x_j) - \frac{1}{|S_j|}\int_{S_j} R_j\varphi dx\right| + \frac{1}{|S_j|}\left|\int_{S_j} R_j\varphi dx\right| \\ &\leq C h_j \|\nabla R_j\varphi\|_{L^\infty(S_j)} + \frac{1}{|S_j|}\left|\int_{S_j}\varphi dx\right| \\ &\leq C\|\nabla R_j\varphi\|_{L^2(S_j)} + C h_j^{-1}\|\varphi\|_{L^2(S_j)} \\ &\leq C\|\nabla\varphi\|_{L^2(S_j)}, \end{aligned}$$

where h_j is the diameter of S_j which is bounded by Ch_K. Here we have used the scaling argument and Poincaré inequality in the last inequality since φ vanishes in part of the boundary of S_j. Thus

$$\|\Pi_h^0\varphi - \Pi_h\varphi\|_{L^2(K)} \leq \sum_{x_j\in N(K)} |(R_j\varphi)(x_j)|\,\|\psi_j\|_{L^2(K)} \leq C h_K \|\nabla\varphi\|_{L^2(\tilde{K})}.$$

To show (9), we only consider the case when K is an immersed boundary element since otherwise, the estimate is a direct consequences of (8) by the scaled trace inequality (see e.g. the argument in [9, Theorem 4.1]). If K is an immersed boundary element and $e \in \mathcal{E}(K)$, by the definition of $h_{e,\Gamma}$, we could put e in a tube T_e of width $h_{e,\Gamma}$ along Γ in which φ vanishes in part of its boundary. Since $\Pi_h^0\varphi = 0$ on e, we easily obtain the estimates

$$\|\varphi - \Pi_h^0\varphi\|_{L^2(e)} = \|\varphi\|_{L^2(e)} \le C\tilde{h}_e^{1/2}\|\nabla\varphi\|_{L^2(T_e)} \le C\tilde{h}_e^{1/2}\|\nabla\varphi\|_{L^2(\tilde{e})},$$

where in the last estimate we have used the local uniformity of elements in $\mathcal{M}_h$. This completes the proof. □

Now we introduce the local error indicator η_K on $K \in \mathcal{M}_h$

$$\eta_K^2 = h_K^2\|f\|_{L^2(K)}^2 + \sum_{e\in\mathcal{E}(K)} \tilde{h}_e\|[\![\nabla u_h \cdot \mathbf{n}]\!]_e\|_{L^2(e)}^2,$$

where $[\![\nabla u_h \cdot \mathbf{n}]\!]_e$ is the jump of discrete flux across e.

In the following theorem, we derive the upper bound of $\|u - u_h\|_{H^1(\Omega)}$ in terms of η_K and $g - u_h$ on the boundary.

Theorem 2.5. *Let u and u_h be the solution of* (5) *and* (6)*, respectively. There exists a constant $C > 0$ depending only on the minimum angle of $\mathcal{M}_h$ such that*

$$\|u - u_h\|_{H^1(\Omega)} \le C\|g - u_h\|_{H^{1/2}(\Gamma)} + C\left(\sum_{K\in\mathcal{M}_h}\eta_K^2\right)^{1/2}.$$

Proof. For any $\varphi \in H_0^1(\Omega)$ which we extend to be zero outside Ω, by (5) we have

$$\begin{aligned}(\nabla(u-u_h),\nabla\varphi) &= \int_\Omega f\varphi dx - \int_\Omega \nabla u_h\cdot\nabla\varphi dx\\ &= \int_{\Omega_h} f\varphi dx - \int_{\Omega_h}\nabla u_h\cdot\nabla\varphi dx\\ &= \int_{\Omega_h} f(\varphi - \Pi_h^0\varphi)dx - \int_{\Omega_h}\nabla u_h\cdot\nabla(\varphi-\Pi_h^0\varphi)dx,\end{aligned}$$

where Π_h^0 is the modified Clément interpolation operator defined in (7) and we have used (6). Now since φ and $\Pi_h^0\varphi$ are zero outside Ω we have

$$(\nabla(u-u_h),\nabla\varphi) = \sum_{K\in\mathcal{M}_h}\int_K f(\varphi-\Pi_h^0\varphi)dx - \sum_{K\in\mathcal{M}_h}\int_{K\cap\Omega}\nabla u_h\cdot\nabla(\varphi-\Pi_h^0\varphi)dx,$$

which by integration by parts, Lemmas 2.4, and standard argument in a posteriori error analysis, implies that

$$\begin{aligned}(\nabla(u-u_h),\nabla\varphi) &= \sum_{K\in\mathcal{M}_h}\int_K f(\varphi-\Pi_h^0\varphi)dx - \sum_{e\in\mathcal{B}_h}\int_e[\![\nabla u_h\cdot\mathbf{n}]\!]_e(\varphi-\Pi_h^0\varphi)dx\\ &\le C\left(\sum_{K\in\mathcal{M}_h}\eta_K^2\right)^{1/2}\|\nabla\varphi\|_{L^2(\Omega)}.\end{aligned}$$

Let $\zeta \in H^1(\Omega)$ be any function that satisfies $\zeta = u - u_h = g - u_h$ on Γ. By taking $\varphi = u - u_h - \zeta \in H_0^1(\Omega)$ in above equality we obtain

$$\|u-u_h\|_{H^1(\Omega)} \le C\|\zeta\|_{H^1(\Omega)} + C\left(\sum_{K\in\mathcal{M}_h}\eta_K^2\right)^{1/2}.$$

This completes the proof since ζ is an arbitrary function that equals to $g - u_h$ on the boundary. □

To consider the local lower bound of $\|u-u_h\|_{H^1(\Omega)}$, we define the local oscillation for $K \in \mathcal{M}_h$ as

$$\mathrm{osc}_K = h_K \|f - f_{\tilde{K}}\|_{L^2(\tilde{K})},$$

where $f_{\tilde{K}} = \frac{1}{|\tilde{K}\cap\Omega|}\int_{\tilde{K}\cap\Omega} f dx$ and $\tilde{K}$ is the union of all elements having non-empty intersection with K. We assume for each immersed boundary element $K \in \mathcal{M}_h$, there exists an element $K' \subset \tilde{K}$ which is entirely contained in Ω. This assumption is not very restrictive if the mesh is sufficiently refined near the boundary.

Theorem 2.6. *There exists a constant $C > 0$ which depends only on the minimum angle of $\mathcal{M}_h$ such that*

$$Ch_K^2\|f\|^2_{L^2(K)} \le \|\nabla(u-u_h)\|^2_{L^2(\tilde{K})} + \mathrm{osc}_K^2, \quad \forall K \in \mathcal{M}_h,$$

$$C\tilde{h}_e\|[\![\nabla u_h \cdot \mathbf{n}]\!]_e\|^2_{L^2(e)} \le \frac{\tilde{h}_e}{\rho_e}\|\nabla(u-u_h)\|^2_{L^2(K_1\cup K_2)} + \mathrm{osc}_K^2, \quad \forall e \in \mathcal{B}_h, e = K_1 \cap K_2,$$

where $\rho_e = \min(\rho_{K_1}, \rho_{K_2})$ and ρ_{K_i} denotes the radius of the largest interior ball of K_i. K_i $(i = 1, 2)$ can be either an element in $\mathcal{M}_h$ or a sub-triangle inside some immersed boundary element.

Proof. We only consider the case when K is an immersed boundary element and $e \in \mathcal{E}(K)$ since otherwise, the estimate follows from the standard argument (see e.g. [9]).

1°) For the immersed boundary element K, we assume $K' \in \tilde{K}$ is contained in Ω. Then

$$\begin{aligned}
h_K^2\|f\|^2_{L^2(K)} &\le 2h_K^2\|f_{\tilde{K}}\|^2_{L^2(K)} + 2h_K^2\|f - f_{\tilde{K}}\|^2_{L^2(K)} \\
&\le 2h_K^2\|f_{\tilde{K}}\|^2_{L^2(\tilde{K})} + 2h_K^2\|f - f_{\tilde{K}}\|^2_{L^2(\tilde{K})} \\
&\le Ch_{K'}^2\|f_{\tilde{K}}\|^2_{L^2(K')} + 2h_K^2\|f - f_{\tilde{K}}\|^2_{L^2(\tilde{K})} \\
&\le Ch_{K'}^2\|f\|^2_{L^2(K')} + Ch_K^2\|f - f_{\tilde{K}}\|^2_{L^2(\tilde{K})} \\
&\le C\|\nabla(u-u_h)\|^2_{L^2(\tilde{K})} + Ch_K^2\|f - f_{\tilde{K}}\|^2_{L^2(\tilde{K})},
\end{aligned}$$

where we have applied the standard argument of lower bound on K' in the last estimate.

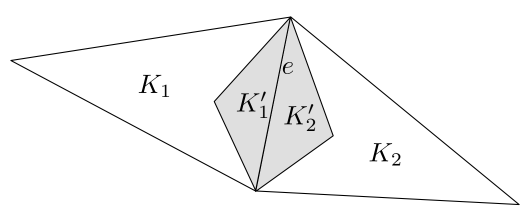

FIGURE 3. Bubble function associated with e.

2°) For any side $e \in \mathcal{B}_h$, let $\psi_e = 4\lambda_1'\lambda_2'$ be the bubble function supported in $K_1' \cup K_2'$, where $K_i' \subset K_i$ is a triangle with e as one of its sides and ρ_{K_i} as the height on e (See Fig. 3 for an illustration), λ_i' are barycentric coordinate functions associated with the nodes of e. We denote $J_e = [\![\nabla u_h \cdot \mathbf{n}]\!]_e$ for short. Denote by $\psi = \beta_e\psi_e$ the function satisfies

$$\int_e J_e\ \psi = \tilde{h}_e\|J_e\|^2_{L^2(e)}.$$

It is easy to check that

$$|\beta_e| \le C\left(\frac{\tilde{h}_e}{h_e}\right)^{1/2}\tilde{h}_e^{1/2}\|J_e\|_{L^2(e)},$$

and thus

$$h_K^{-1}\|\psi\|_{L^2(K_1'\cup K_2')} \le C\tilde{h}_e^{1/2}\|J_e\|_{L^2(e)}, \quad \|\nabla\psi\|_{L^2(K_1'\cup K_2')} \le C\left(\frac{\tilde{h}_e}{\rho_e}\right)^{1/2}\tilde{h}_e^{1/2}\|J_e\|_{L^2(e)}.$$

By (5) and (6), since $\psi \in H_0^1(K_1 \cup K_2)$, we have

$$\begin{aligned}\tilde{h}_e\|J_e\|^2_{L^2(e)} &= \int_e J_e\ \psi = \int_{K_1'\cup K_2'} f\psi dx - \int_{K_1'\cup K_2'}\nabla(u-u_h)\nabla\psi dx \\ &\le C\tilde{h}_e^{1/2}\|J_e\|_{L^2(e)}\left(h_K^2\|f\|^2_{L^2(K_1\cup K_2)} + \frac{\tilde{h}_e}{\rho_e}\|\nabla(u-u_h)\|^2_{L^2(K_1\cup K_2)}\right)^{\frac{1}{2}}.\end{aligned}$$

This completes the proof upon using the estimate for $h_K\|f\|_{L^2(K)}$. □

To localize the global upper bound $\|g-u_h\|_{H^{1/2}(\Gamma)}$, we recall the following theorem of Faermann [15, Corollary 2.3].

Lemma 2.7. *Let I be an arbitrary finite index set and $\{v_q\}_{q\in I} \subset H^{1/2}(\Gamma)$ with weakly disjoint supports, that is, the measure $|\mathrm{supp}(v_p)\cap\mathrm{supp}(v_q)| = 0$ for all $p, q \in I, p \ne q$. Then there exists a constant C independent of the index set I such that*

$$C^{-1}\sum_{q\in I}\|v_q\|^2_{H^{1/2}(\Gamma)} \le \Big\|\sum_{q\in I} v_q\Big\|^2_{H^{1/2}(\Gamma)} \le C\sum_{q\in I}\|v_q\|^2_{H^{1/2}(\Gamma)}.$$

If $g \in C(\Gamma)$ and g_h is the Lagrange interpolation of g on Γ_h, then $g-u_h$ vanishes at the intersection points of K and Γ. Thus by combing Theorem 2.5 and Lemma 2.7 we have

$$\|g-u_h\|_{H^{1/2}(\Gamma)} \le C\left(\sum_{K\in\mathcal{M}_h}\|g-u_h\|^2_{H^{1/2}(K\cap\Gamma)}\right)^{1/2}.$$

By the definition of the Sobolev-Slobodeckij norm of order 1/2 we obtain the following upper bound when $g = 0$ which will be used in our computations.

Corollary 2.8. *Let $g = 0$ in Γ. We have*

$$\|u_h\|_{H^{1/2}(\Gamma)} \le C\left(\sum_{K\in\mathcal{M}_h} h_K\|\nabla u_h\|^2_{L^2(K\cap\Gamma)}\right)^{1/2}.$$

To conclude this section we give some remarks. The constant $\frac{\tilde{h}_e}{\rho_e}$ appearing in Theorem 2.6 could deteriorate the efficiency of jump residual for some sub-triangles (see left case of Fig 4 for an example in which K_2 comparing with K_1 is much too narrow in shape). We note that $\frac{\tilde{h}_e}{\rho_e}$ will not blow up even for flat sub-triangles (see right case of Fig 4) and the lower bounds of residue in Theorem 2.6 do not depend on such constant. This problem is not very serious in the practical applications of using the error indicator for the mesh adaptation since it leads to possible over-refinement only for immersed boundary elements.

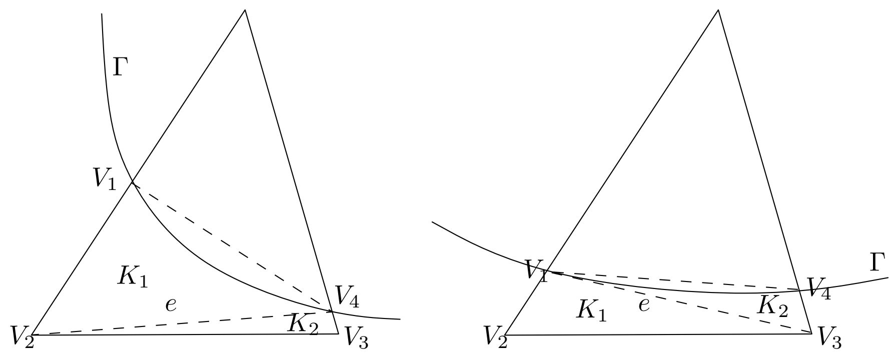

FIGURE 4. The constant $\frac{\tilde{h}_e}{\rho_e}$ in the lower bound of (10) may blow up in the left case while stays safe for the right.

It is somewhat inconvenient to calculate $\tilde{h}_e$ in practical applications. In our implementations we use the following enlarged a posteriori error indicator

$$\tilde{\eta}_K^2 = h_K^2 \|f\|_{L^2(K)}^2 + \sum_{e \in \mathcal{E}(K)} h_K \|[\![\nabla u_h \cdot \mathbf{n}]\!]_e\|_{L^2(e)}^2,$$

The upper bound of Theorem 2.5 is still valid if η_K is replaced by $\tilde{\eta}_K$.

3. The arbitrary Lagrangian-Eulerian scheme

Let $G(0,T) = \{(x,t) : \ x \in \Omega(t), t \in (0,T)\}$ be the space time domain which we assume is Lipschitz. Given $f \in L^2(0,T,H^{-1}(\Omega(t)))$ and $u_0 \in L^2(\Omega(0))$, the weak formulation of the problem (1)-(3) is to find

$$u \in L^2(0,T,H_0^1(\Omega(t))) \cap H^1(0,T,H^{-1}(\Omega(t)))$$

such that $u = u_0$ in $\Omega(0)$ and for a.e. $t \in (0,T)$

$$\langle \partial_t u, v\rangle_{\Omega(t)} + (\nabla u, \nabla v)_{\Omega(t)} = \langle f, v\rangle_{\Omega(t)}, \quad \forall v \in H_0^1(\Omega(t)), \tag{10}$$

where $\langle \cdot,\cdot\rangle_{\Omega(t)}$ is the duality pairing between $H^{-1}(\Omega(t))$ and $H_0^1(\Omega(t))$ and $(\cdot,\cdot)_{\Omega(t)}$ is the inner product of $L^2(\Omega(t))$. The uniqueness and existence of the weak solution can be proved by extending the Galerkin method for parabolic problems in cylindrical space time domains. Here we omit the details. For simplicity we assume in the following that $f \in C(0,T;L^2(\Omega(t)))$.

Let τ_n be the n-th time step size and set

$$t^n := \sum_{i=1}^n \tau_i, \quad \varphi^n(\cdot) = \varphi(\cdot, t^n),$$

for any function φ continuous in time. Let N be the total number of time steps, that is, $t^N \ge T$. We assume there are constants C_1 and C_2 such that $C_1\tau_{n-1} \le \tau_n \le C_2\tau_{n-1}$, $n = 1, \cdots, N$.

Now we introduce the ALE time discretization scheme for the problem (10). Let $F_t : \hat{\Omega} \to \Omega(t)$ be the bijective map which for any $t \in (0,T)$, maps the reference domain $\hat{\Omega}$ to $\Omega(t)$. Denote $F_t^{-1} : \Omega(t) \to \hat{\Omega}$ the inverse map of F_t. We assume $F(\hat{x},t) = F_t(\hat{x})$ and $F^{-1}(x,t) = F_t^{-1}(x)$ are Lipschitz continuous in $G(0,T)$. For any function $v(x,t)$ defined in $\Omega(t)$, we will use the notation $\hat{v}(\hat{x},t) = v\left(F_t(\hat{x}),t\right)$

to denote the pullback of v to $\hat{\Omega}$. Then for the solution u of the problem (10) we have

$$\partial_t \hat{u}(\hat{x},t) = \partial_t u\left(F_t(\hat{x}),t\right) + \nabla u\left(F_t(\hat{x}),t\right) \cdot \partial_t F_t(\hat{x},t) \quad \text{in } \hat{\Omega},$$

and the equation (1) transforms to

$$\partial_t \hat{u} - \nabla u\left(F_t(\hat{x}),t\right) \cdot \partial_t F_t(\hat{x}) - \hat{\Delta}\hat{u} = \hat{f} \quad \text{in } \hat{\Omega}, \tag{11}$$

where $\hat{\Delta}\hat{u} = J^{-1}\widehat{\mathrm{div}}\left[J(\hat{D}F_t)^{-1}(\hat{D}F_t)^{-T}\hat{\nabla}\hat{u}\right]$ is the transformed Laplacian in the reference domain $\hat{\Omega}$, $\hat{D}F_t$ is the gradient matrix of the map F_t, and $J(\hat{x}) = \det(\hat{D}F_t(\hat{x}))$. The implicit Euler scheme for (11) at $t = t^n$ is

$$\frac{\hat{U}^n - \hat{U}^{n-1}}{\tau_n} - \nabla U^n(F_{t^n}(\hat{x})) \cdot (\partial_t F_t)|_{t=t^n}(\hat{x}) - \hat{\Delta}\hat{U}^n = \hat{f}^n \quad \text{in } \hat{\Omega},$$

which yields the following ALE scheme after transforming the equation back to $\Omega^n = \Omega(t^n)$

$$\frac{U^n - \bar{U}^{n-1}}{\tau_n} - \mathbf{v}^n \cdot \nabla U^n - \Delta U^n = f^n \quad \text{in } \Omega^n, \tag{12}$$

where $\bar{U}^{n-1}$ and $\mathbf{v}^n$ are defined by

$$\bar{U}^{n-1} = U^{n-1}(F_{t^{n-1}}(F_{t^n}^{-1}(x))), \quad \mathbf{v}^n = (\partial_t F_t)|_{t=t^n}(F_{t^n}^{-1}(x)), \quad \forall x \in \Omega^n. \tag{13}$$

Let Ω be a polygonal domain such that $\Omega(t) \subset \Omega$ for any $t \in (0,T)$ and $\mathcal{M}_h$ the shape regular triangulation of Ω. We will use the immersed finite element method in section 2 to discretize the elliptic problem (12) at each time step. We will always assume the mesh $\mathcal{M}^n$ at time t^n is a refinement of a subset of elements in $\mathcal{M}_h$. Thus the consecutive meshes at two time steps are *compatible* in the sense that $\mathcal{M}^n$ is obtained from $\mathcal{M}^{n-1}$ by refinement/corasening procedures.

Let Ω_h^n be a polygonal domain such that $\Omega^n \subset \Omega_h^n$. Let $\mathcal{M}^n$ be a regular triangulation of Ω_h^n and $V_h^n(\Omega_h^n)$ the immersed finite element space defined in section 2. Denote $\overset{\circ}{V}{}_h^n(\Omega_h^n)$ the set of all functions in $V_h^n(\Omega_h^n)$ that vanish at all degrees of freedom on Γ_h^n and outside Ω^n. The functions in $\overset{\circ}{V}{}_h^n(\Omega_h^n)$ are supported in $\tilde{\Omega}_h^n = \Omega_h^n \backslash \bar{\Omega}_h^{n,\mathrm{out}}$, where $\Omega_h^{n,\mathrm{out}}$ is the union of all sub-triangles of the immersed boundary elements in $\mathcal{M}^n$ which have at least one vertex outside $\bar{\Omega}^n$. We also denote $I_h^n : C(\bar{\Omega}) \to V_h^n(\Omega_h^n)$ the standard Lagrangian interpolation operator.

The immersed finite element approximation at the n-th time step reads as follows: Given $U_h^{n-1} \in \overset{\circ}{V}{}_h^{n-1}(\Omega_h^{n-1})$ which we extend to be zero outside Ω_h^{n-1}, then $\mathcal{M}^{n-1}$ and τ_{n-1} are modified as described below to give rise to $\mathcal{M}_h^n$ and τ_n and thereafter $U_h^n \in \overset{\circ}{V}{}_h^n(\Omega_h^n)$ computed according to the following prescription, for any $v_h^n \in \overset{\circ}{V}{}_h^n(\Omega_h^n)$,

$$\begin{aligned}(U_h^n, v_h^n)_{\Omega_h^n} - (\bar{U}_h^{n-1}, v_h^n)_{\Omega_h^n} - \tau_n(\mathbf{v}^n \cdot \nabla U_h^n, v_h^n)_{\Omega_h^n} \quad &+ \quad \tau_n(\nabla U_h^n, \nabla v_h^n)_{\Omega_h^n} \\ &= \quad \tau_n(f^n, v_h^n)_{\Omega_h^n}.\end{aligned} \tag{14}$$

Here we extend f^n to be zero outside Ω^n and define $\bar{U}_h^{n-1}(x) = U_h^{n-1}(F_{t^{n-1}}(F_{t^n}^{-1}(x)))$ for $x \in \Omega^n$ and $\bar{U}_h^{n-1}(x) = 0$ for $x \in \Omega_h^n \backslash \bar{\Omega}^n$.

The discrete problem (14) is obviously well-defined. One can also derive a priori error estimates for the solution (14) by using the energy argument and the results in Section 2. In this paper we are interested in the a posteriori error estimate and developing adaptive finite element method for solving the problem (10). We leave the a priori error analysis to the interested readers.

To conclude this section we recall Hadamard formula which will be used in the subsequent analysis. Assume that the space time domain $G(0,T)$ is defined by a level set function Φ which is Lipschitz in $\mathbb{R}^3$ such that

$$\Phi(x,t)<0 \ \text{ in } \Omega(t), \quad \Phi(x,t)=0 \ \text{ on } \Gamma(t), \quad \Phi(x,t)>0 \ \text{ in } \mathbb{R}^2\backslash\overline{\Omega(t)}.$$

We assume the level set function does not degenerate at each time t, that is, $|\nabla_x\Phi|>0$ on $\Gamma(t)$ for any $t\in(0,T)$. The following lemma is a generalization of the classical Hadamard formula [2].

Lemma 3.1. *Let $G(0,T)$ have Lipschitz boundary. Assume that*

$$f,\partial_t f\in L^\infty(0,T;L^1(\Omega(t))), \quad f\in L^\infty(0,T;L^1(\Gamma(t))).$$

Then we have

$$\frac{d}{dt}\int_{\Omega(t)} f dx=\int_{\Omega(t)}\frac{\partial f}{\partial t}dx-\int_{\Gamma(t)} f\frac{\partial_t\Phi}{|\nabla_x\Phi|}ds_x, \quad a.e.\ t\in(0,T). \tag{15}$$

Proof. For the sake of completeness we include a proof here. For any fixed $t_0\in(0,T)$ and an arbitrary small number $\epsilon>0$, by using integration by parts we have

$$\begin{aligned}\int_{t_0}^{t_0+\epsilon}\int_{\Omega(t)}\frac{\partial f}{\partial t}dxdt &= \int_{\Omega(t_0+\epsilon)} fdx-\int_{\Omega(t_0)} fdx+\int_{t_0}^{t_0+\epsilon}\int_{\Gamma(t)} fn_t ds_{(x,t)}\\ &= \int_{\Omega(t_0+\epsilon)} fdx-\int_{\Omega(t_0)} fdx+\int_{t_0}^{t_0+\epsilon}\int_{\Gamma(t)} fn_t\frac{|\nabla\Phi|}{|\nabla_x\Phi|}ds_x dt,\end{aligned}$$

where n_t is the time component of the unit normal to $\partial G(0,T)$ and $\nabla\Phi=(\nabla_x\Phi,\partial_t\Phi)^T$ is the gradient in the space time domain. Since $n_t=\partial_t\Phi/|\nabla\Phi|$ by the property of the level set function, we know that

$$\int_{t_0}^{t_0+\epsilon}\int_{\Omega(t)}\frac{\partial f}{\partial t}dxdt=\int_{\Omega(t_0+\epsilon)} fdx-\int_{\Omega(t_0)} fdx+\int_{t_0}^{t_0+\epsilon}\int_{\Gamma(t)} f\frac{\partial_t\Phi}{|\nabla_x\Phi|}ds_x dt.$$

The lemma follows by dividing the above equation by ϵ and letting ϵ tend to 0. $\square$

In our case $\Gamma(t)$ is a mapping of some reference boundary $\hat\Gamma$, $x=F_t(\hat x)$ for $x\in\Gamma(t)$ and $\hat x\in\hat\Gamma$, we have $\Phi(F_t(\hat x),t)=0$ on $\hat\Gamma$. Thus

$$(\nabla_x\Phi)(F_t(\hat x),t)\cdot\partial_t F_t(\hat x)+(\partial_t\Phi)(F_t(\hat x),t)=0.$$

Let $\mathbf{v}(x,t)=(\partial_t F_t)(F_t^{-1}(x))$ be the moving velocity of the boundary $\Gamma(t)$. Then we deduce from Lemma 3.1 that

$$\frac{d}{dt}\int_{\Omega(t)} fdx=\int_{\Omega(t)}\frac{\partial f}{\partial t}dx+\int_{\Gamma(t)} f(\mathbf{v}\cdot\mathbf{n}_x)ds_x,$$

where $\mathbf{n}_x=\nabla_x\Phi/|\nabla_x\Phi|$ is the unit outer normal to $\Gamma(t)$ in the plane occupied by $\Omega(t)$. This is the classical form of the Hadamard formula.

4. A posteriori error analysis

For any $\hat x\in\hat\Omega$, let $\hat U_h^n(\hat x)=U_h^n(F_{t^n}(\hat x))$, $1\le n\le N$, which is well-defined since $\Omega^n\subset\Omega_h^n$. We define

$$U_h(x,t)=l(t)\hat U_h^n(F_t^{-1}(x))+(1-l(t))\hat U_h^{n-1}(F_t^{-1}(x))), \quad \forall x\in\Omega(t),\forall t^{n-1}\le t\le t^n,$$

where $l(t)=(t-t_{n-1})/\tau_n$.

The following estimate is the starting point of the a posteriori error estimation in this section.

Lemma 4.1. *Let*

$$f_1(x,t) := \frac{\partial(u-U_h)}{\partial t} - \Delta(u-U_h) \quad \text{in } H^{-1}(\Omega(t)) \quad \text{a.e. in } (0,T). \tag{16}$$

Then there exists a constant C independent of T such that

$$\begin{aligned}
&\max_{0\le t\le T}\|u-U_h\|^2_{L^2(\Omega(t))} + \int_0^T \|\nabla(u-U_h)\|^2_{L^2(\Omega(t))}dt \\
\le\ & \|u_0 - U_h^0\|^2_{L^2(\Omega(0))} + C\max_{0\le t\le T}\|\zeta\|^2_{L^2(\Omega(t))} \\
+\ & C\int_0^T \left(\|f_1\|^2_{H^{-1}(\Omega(t))} + \|\partial_t\zeta\|^2_{H^{-1}(\Omega(t))} + \|\nabla\zeta\|^2_{L^2(\Omega(t))}\right)dt,
\end{aligned} \tag{17}$$

where $\zeta \in L^2(0,T;H^1(\Omega(t))) \cap H^1(0,T;H^{-1}(\Omega(t)))$ be any function such that $\zeta = u - U_h = -U_h$ on $\Gamma(t)$, a.e. $t \in (0,T)$.

Proof. We use the standard energy argument. We multiply (16) by $v = u-U_h-\zeta \in H_0^1(\Omega(t))$ and use Lemma 3.1 to obtain

$$\begin{aligned}
&\frac{1}{2}\frac{d}{dt}\|u-U_h-\zeta\|^2_{L^2(\Omega(t))} + \|\nabla(u-U_h-\zeta)\|^2_{L^2(\Omega(t))} \\
=\ & \langle f_1 - \partial_t\zeta, u-U_h-\zeta\rangle_{\Omega(t)} - (\nabla\zeta, \nabla(u-U_h-\zeta))_{\Omega(t)} \\
\le\ & C\left(\|f_1-\partial_t\zeta\|_{H^{-1}(\Omega(t))} + \|\nabla\zeta\|_{L^2(\Omega(t))}\right)\|\nabla(u-U_h-\zeta)\|_{L^2(\Omega(t))}.
\end{aligned}$$

By Cauchy-Schnwarz inequality we obtain easily

$$\begin{aligned}
&\max_{0\epsilon t\le T}\|u-U_h-\zeta\|^2_{L^2(\Omega(t))} + \int_0^T \|\nabla(u-U_h-\zeta)\|^2_{L^2(\Omega(t))}dt \\
\le\ & \|u_0 - U_h^0 - \zeta_0\|^2_{L^2(\Omega(0))} \\
& + C\int_0^T \left(\|f_1\|^2_{H^{-1}(\Omega(t))} + \|\partial_t\zeta\|^2_{H^{-1}(\Omega(t))} + \|\nabla\zeta\|^2_{L^2(\Omega(t))}\right)dt,
\end{aligned}$$

The proof follows from the triangle inequality. □

ζ is the parabolic extension of the boundary value $-U_h$ on $\Gamma(t)$ whose estimation is our next goal. We first recall the following theorem of Verchota [21, Theorem 2.2.22].

Lemma 4.2. *Let D be a bounded Lipschitz domain in R^d, $d \ge 2$, with D and $\mathbb{R}^d\backslash\bar{D}$ connected. There exists $\varepsilon > 0$, which depends only on the Lipschitz character of D such that $\frac{1}{2}I + K$ is invertible from $L^p(\partial D)$ to itself, where K is the operator on ∂D given by*

$$Kg(x) = \frac{1}{\omega_d}\int_{\partial D}\frac{\langle x-y, \mathbf{n}(y)\rangle}{|x-y|^d}g(y)ds(y).$$

Here ω_d is the surface area of the unit sphere in $\mathbb{R}^d$ and $\mathbf{n}$ is the unit outer normal to ∂D. Consequently, the solution to Dirichlet problem $-\Delta u = 0$ in D with boundary condition $u = g$ on ∂D, where $g \in L^p(\partial D), 2-\varepsilon < p < \infty$, can be represented as

$$u(x) = \frac{1}{\omega_d}\int_{\partial D}\frac{\langle x-y, \mathbf{n}(y)\rangle}{|x-y|^d}\left(\frac{1}{2}I + K\right)^{-1}(g)ds(y).$$

For any $1 \le n \le N$, $t^{n-1} \le t \le t^n$, let $\hat{\zeta}^n(\hat{x},t) \in H^1(\hat{\Omega})$ be the weak solution of the Dirichlet problem

$$-\Delta\hat{\zeta}^n = 0 \ \text{ in } \hat{\Omega}, \qquad \hat{\zeta}^n = -\left[l(t)\hat{U}_h^n + (1-l(t))\hat{U}_h^{n-1}\right] \ \text{ on } \hat{\Gamma}. \tag{18}$$

By Lax-Milgram lemma, $\hat{\zeta}^n$ is uniquely existent. We define

$$\zeta(x,t)=\hat{\zeta}^n(F_t^{-1}(x),t),\quad \forall x\in\Omega(t), t^{n-1}\le t\le t^n, n=1,\cdots,N.$$

It is clear that $\zeta=-U_h$ on $\Gamma(t)$, a.e. $t\in(0,T)$.

Lemma 4.3. *There exists a constant $C>0$ independent of T such that*

$$\begin{aligned}&\max_{0\le t\le T}\|\zeta\|^2_{L^2(\Omega(t))}+\int_0^T\left(\|\partial_t\zeta\|^2_{H^{-1}(\Omega(t))}+\|\nabla\zeta\|^2_{L^2(\Omega(t))}\right)dt\\ \le\ & CT\max_{0\le n\le N}\left(\sum_{K\in\mathcal{M}^n}h_K\|\nabla U_h^n\|^2_{L^2(K\cap\Gamma^n)}\right)+C\sum_{n=1}^N\tau_n\|(U_h^n-\bar{U}_h^{n-1})/\tau_n\|^2_{L^2(\Gamma^n)}.\end{aligned}$$

Proof. For $t\in[t^{n-1},t^n]$, notice that

$$\partial_t\zeta(x,t)=\partial_t\hat{\zeta}^n(F_t^{-1}(x),t)+\hat{\nabla}\hat{\zeta}^n(F_t^{-1}(x),t)\cdot\partial_tF_t^{-1}(x),\quad\forall x\in\Omega(t),$$

we obtain, since F_t and F_t^{-1} are Lipschitz continuous,

$$\begin{aligned}\|\partial_t\zeta\|_{H^{-1}(\Omega(t))}&\le C\|\partial_t\hat{\zeta}^n\|_{H^{-1}(\hat{\Omega})}+C\|\hat{\nabla}\hat{\zeta}^n\|_{L^2(\hat{\Omega})}\\&\le C\|\partial_t\hat{\zeta}^n\|_{H^{-1}(\hat{\Omega})}+C\|\nabla\zeta\|_{L^2(\Omega(t))}.\end{aligned}$$

On the other hand, again by the Lipschitz continuity of F_t and F_t^{-1}, we have

$$\begin{aligned}\|\zeta\|_{H^1(\Omega(t))}\le C\|\hat{\zeta}^n\|_{H^1(\hat{\Omega})}&\le C\left(\|\hat{U}_h^n\|_{H^{1/2}(\hat{\Gamma})}+\|\hat{U}_h^{n-1}\|_{H^{1/2}(\hat{\Gamma})}\right)\\&\le C\left(\|U_h^n\|_{H^{1/2}(\Gamma^n)}+\|U_h^{n-1}\|_{H^{1/2}(\Gamma^{n-1})}\right).\end{aligned}$$

By Corollary 2.8 we have

$$\|U_h^n\|_{H^{1/2}(\Gamma^n)}\le C\left(\sum_{K\in\mathcal{M}^n}h_K\|\nabla U_h^n\|^2_{L^2(K\cap\Gamma^n)}\right)^{1/2}.\tag{19}$$

Thus we only remain to estimate $\|\partial_t\hat{\zeta}^n\|_{H^{-1}(\hat{\Omega})}$. By Lemma 4.2 we know that there exists a function $\hat{g}\in L^2(\hat{\Gamma})$ such that $\|\hat{g}\|_{L^2(\hat{\Gamma})}\le C\|(\hat{U}_h^n-\hat{U}_h^{n-1})/\tau_n\|_{L^2(\hat{\Gamma})}$ and

$$\partial_t\hat{\zeta}^n=\frac{1}{2\pi}\int_{\hat{\Gamma}}\frac{(\hat{x}-\hat{y})\cdot\hat{\mathbf{n}}(\hat{y})}{|\hat{x}-\hat{y}|^2}\hat{g}(\hat{y})ds(\hat{y}).$$

Thus, for any $\hat{v}\in H_0^1(\hat{\Omega})$,

$$\begin{aligned}\langle\partial_t\hat{\zeta}^n,\hat{v}\rangle_{\hat{\Omega}}&=\frac{1}{2\pi}\int_{\hat{\Omega}}\int_{\hat{\Gamma}}\frac{(\hat{x}-\hat{y})\cdot\hat{\mathbf{n}}(\hat{y})}{|\hat{x}-\hat{y}|^2}\hat{g}(\hat{y})\hat{v}(\hat{x})ds(\hat{y})d\hat{x}\\&\le C\|\hat{g}\|_{L^2(\hat{\Gamma})}\left\|\int_{\hat{\Omega}}\frac{(\hat{x}-\hat{y})\cdot\hat{\mathbf{n}}(\hat{y})}{|\hat{x}-\hat{y}|^2}\hat{v}d\hat{x}\right\|_{L^2(\hat{\Gamma})}.\end{aligned}$$

On the other hand, it is easy to see that for any $p>2$,

$$\left|\int_{\hat{\Omega}}\frac{(\hat{x}-\hat{y})\cdot\hat{\mathbf{n}}(\hat{y})}{|\hat{x}-\hat{y}|^2}\hat{v}d\hat{x}\right|\le C\|\hat{v}\|_{L^p(\hat{\Omega})}\le C\|\hat{v}\|_{H^1(\hat{\Omega})},\qquad\forall\hat{y}\in\hat{\Gamma},$$

where we have used the Sobolev embedding theorem in the last estimate. This shows that

$$\begin{aligned}\|\partial_t\hat{\zeta}^n\|_{H^{-1}(\hat{\Omega})}&\le C\|\hat{g}\|_{L^2(\hat{\Gamma})}\le C\|(\hat{U}_h^n-\hat{U}_h^{n-1})/\tau_n\|_{L^2(\hat{\Gamma})}\\&\le C\|(U_h^n-\bar{U}_h^{n-1})/\tau_n\|_{L^2(\Gamma^n)}.\end{aligned}$$

This completes the proof. □

The following theorem is the main result of this paper.

Theorem 4.4. *There exists a constant C depending only on the minimum angles of $\mathcal{M}^n$, $n = 1, \cdots, N$, such that*

$$\begin{aligned}
&\max_{0\le t\le T} \|u - U_h\|^2_{\Omega(t)} + \int_0^T \|\nabla(u - U_h)\|^2_{L^2(\Omega(t)))} dt \\
\le\ & \|u_0 - U_h^0\|^2_{L^2(\Omega(0))} + CT \max_{0\le n\le N} \left(\sum_{K\in\mathcal{M}^n} h_K \|\nabla U_h^n\|^2_{L^2(K\cap\Gamma^n)} \right) \\
&+ C\sum_{n=1}^N \tau_n \left(\sum_{K\in\mathcal{M}^n} \eta^2_{K,n} \right) + C\sum_{n=1}^N \int_{t^{n-1}}^{t^n} \|f - \tilde{f}^n\|^2_{L^2(\Omega(t))} dt \\
&+ C\sum_{n=1}^N \tau_n \Big(\tau_n^2 \|R^n\|^2_{L^2(\Omega_h^n)} + \tau_n^2 \|\nabla U_h^n\|^2_{L^2(\Omega_h^n)} + \|\nabla(U_h^n - \bar{U}_h^{n-1})\|^2_{L^2(\Omega_h^n)} \\
&\qquad + \|(U_h^n - \bar{U}_h^{n-1})/\tau_n\|^2_{L^2(\Gamma^n)} \Big).
\end{aligned}$$

where $\tilde{f}^n(x,t) = \hat{f}^n(F_t^{-1}(x), t)$ for $x \in \Omega(t), t \in [t^{n-1}, t^n]$, and $\eta_{K,n}$ is the local error indicator defined by

$$\begin{aligned}
\eta^2_{K,n} &= h_K^2 \|R^n\|^2_{L^2(K)} + \sum_{e\in\mathcal{E}(K)} h_K \|[\![\nabla U_h^n \cdot \mathbf{n}]\!]\|^2_{L^2(e)}, \\
R^n &= f^n - \frac{U_h^n - \bar{U}_h^{n-1}}{\tau_n} + \mathbf{v}^n \cdot \nabla U_h^n.
\end{aligned}$$

Proof. From Lemmas 4.1 and 4.3 we only need to estimate $\|f_1\|_{L^2(0,T;H^{-1}(\Omega(t)))}$. For any $t^{n-1} \le t \le t^n$ and $v \in H_0^1(\Omega(t))$, by the equation (1), we have

$$\begin{aligned}
\langle f_1, v\rangle_{\Omega(t)} &= \langle \partial_t(u - U_h), v\rangle_{\Omega(t)} + (\nabla(u - U_h), \nabla v)_{\Omega(t)} \\
&= (f - \tilde{f}^n, v)_{\Omega(t)} + \Big[(\tilde{f}^n - \partial_t U_h, v)_{\Omega(t)} - (\nabla \tilde{U}_h^n, \nabla v)_{\Omega(t)} \Big] \\
&+ (\nabla(\tilde{U}_h^n - U_h), \nabla v)_{\Omega(t)},
\end{aligned} \tag{20}$$

where $\tilde{f}^n, \tilde{U}_h^n$ are functions defined in $\Omega(t)$ given by

$$\tilde{f}^n(x,t) = \hat{f}^n(F_t^{-1}(x)), \quad \tilde{U}_h^n(x,t) = \hat{U}_h^n(F_t^{-1}(x)), \quad \forall x \in \Omega(t).$$

It is easy to see that

$$|(f - \tilde{f}^n, v)_{\Omega(t)}| \le C\|f - \tilde{f}^n\|_{L^2(\Omega(t))} \|\nabla v\|_{L^2(\Omega(t))}. \tag{21}$$

From the definition of $U_h(x,t)$ at the beginning of this section, we know that $\tilde{U}_h^n - U_h = (1 - l(t))(\hat{U}_h^n - \hat{U}_h^{n-1})(F_t^{-1}(x))$. Thus, by the Lipschitz continuity of F_t and F_t^{-1},

$$\|\nabla(\tilde{U}_h^n - U_h)\|_{L^2(\Omega(t))} \le C\|\hat{\nabla}(\hat{U}_h^n - \hat{U}_h^{n-1})\|_{L^2(\hat{\Omega})} \le C\|\nabla(U_h^n - \bar{U}_h^{n-1})\|_{L^2(\Omega_h^n)},$$

which implies

$$|(\nabla(\tilde{U}_h^n - U_h), \nabla v)_{\Omega(t)}| \le C\|\nabla(U_h^n - \bar{U}_h^{n-1})\|_{L^2(\Omega_h^n)} \|\nabla v\|_{L^2(\Omega(t))}. \tag{22}$$

For the remaining term in (20), we first note that for any $v \in H_0^1(\Omega(t))$, $\hat{v}(\hat{x}, t) = v(F_t(\hat{x}), t)$ is in $H_0^1(\hat{\Omega})$, and consequently, $V_n(x,t) := \hat{v}(F_{t^n}^{-1}(x), t)$ belongs to $H_0^1(\Omega^n)$.

It is easy to see that

$$
\begin{aligned}
(23)\qquad & (\tilde{f}^n - \partial_t U_h, v)_{\Omega(t)} - (\nabla \tilde{U}_h^n, \nabla v)_{\Omega(t)} \\
= & \left[(\tilde{f}^n - \partial_t U_h, v)_{\Omega(t)} - (f^n - (\partial_t U_h)(\cdot, t^n), V_n)_{\Omega^n}\right] \\
+ & \left[(f^n - (\partial_t U_h)(\cdot, t^n), V_n)_{\Omega^n} - (\nabla U_h^n, \nabla V_n)_{\Omega^n}\right] \\
+ & \left[(\nabla U_h^n, \nabla V_n)_{\Omega^n} - (\nabla \tilde{U}_h^n, \nabla v)_{\Omega(t)}\right] \\
(24)\qquad =: & \ \mathrm{I} + \mathrm{II} + \mathrm{III}.
\end{aligned}
$$

By the definition of U_h we have

$$
\begin{aligned}
\partial_t U_h(x,t) \ = \ & (\hat{U}_h^n - \hat{U}_h^{n-1})(F_t^{-1}(x))/\tau_n \\
& + \left[l(t)\hat{\nabla}\hat{U}_h^n + (1-l(t))\hat{\nabla}\hat{U}_h^{n-1}\right](F_t^{-1}(x)) \cdot \partial_t F_t^{-1}(x).
\end{aligned}
$$

This yields

$$
\begin{aligned}
& \widehat{\partial_t U_h}(\hat{x}, t) - \widehat{\partial_t U_h}(\hat{x}, t^n) \\
= & \left[l(t)\hat{\nabla}\hat{U}_h^n + (1-l(t))\hat{\nabla}\hat{U}_h^{n-1}\right](\hat{x}) \cdot (\partial_t F_t^{-1})(F_t(\hat{x})) \\
& -\hat{\nabla}\hat{U}_h^n(\hat{x}) \cdot (\partial_t F_t^{-1})(F_t(\hat{x}))|_{t=t^n}.
\end{aligned}
$$

Therefore

$$
\begin{aligned}
\|\widehat{\partial_t U_h}(\hat{x}, t) - \widehat{\partial_t U_h}(\hat{x}, t^n)\|_{L^2(\hat{\Omega})} \ \le \ & C\tau_n \|\hat{\nabla}\hat{U}_h^n\|_{L^2(\hat{\Omega})} + C\|\hat{\nabla}(\hat{U}_h^n - \hat{U}_h^{n-1})\|_{L^2(\hat{\Omega})} \\
(25)\qquad \le \ & C\tau_n \|\nabla U_h^n\|_{L^2(\Omega_h^n)} + C\|\nabla(U_h^n - \bar{U}_h^{n-1})\|_{L^2(\Omega_h^n)}.
\end{aligned}
$$

On the other hand, since $F_t(F_t^{-1}(x)) = x$, by differentiate the identity in time we know that

$$
(\partial_t F_t)(F_t^{-1}(x)) + \hat{D}F_t((F_t^{-1}(x))) \cdot \partial_t F_t^{-1}(x) = 0.
$$

Thus

$$
\begin{aligned}
& (\partial_t U_h)(x, t^n) \\
= \ & (U_h^n - \bar{U}_h^{n-1})/\tau_n + \hat{\nabla}\hat{U}_h^n(F_{t^n}^{-1}(x)) \cdot \partial_t F_t^{-1}|_{t=t^n}(x) \\
= \ & (U_h^n - \bar{U}_h^{n-1})/\tau_n \\
& -\hat{\nabla}\hat{U}_h^n(F_{t^n}^{-1}(x)) \cdot \hat{D}F_t|_{t=t^n}(F_{t^n}^{-1}(x))^{-1} \cdot \partial_t F_t|_{t=t^n}(F_{t^n}^{-1}(x)) \\
(26)\qquad = \ & (U_h^n - \bar{U}_h^{n-1})/\tau_n - \nabla U_h^n \cdot \mathbf{v}^n, \qquad \forall x \in \Omega^n,
\end{aligned}
$$

where $\mathbf{v}^n$ is defined in (13). Now by using (25)-(26) we arrive at

$$
\begin{aligned}
\mathrm{I} \ = \ & \int_{\hat{\Omega}} (\hat{f}^n - \widehat{\partial_t U_h}(\cdot, t^n))\hat{v}(J - J^n) d\hat{x} \\
& - \int_{\hat{\Omega}} (\widehat{\partial_t U_h} - \widehat{\partial_t U_h}(\cdot, t^n))\hat{v} J^n d\hat{x} \\
\le \ & C\tau_n \|\hat{f}^n - \widehat{\partial_t U_h}(\cdot, t^n))\|_{L^2(\hat{\Omega})} \|\hat{v}\|_{L^2(\hat{\Omega})} \\
& + C\|\widehat{\partial_t U_h}(\cdot, t) - \widehat{\partial_t U_h}(\cdot, t^n)\|_{L^2(\hat{\Omega})} \|\hat{v}\|_{L^2(\hat{\Omega})} \\
\le \ & C\Big[\tau_n \|R^n\|_{L^2(\Omega_h^n)} + \tau_n \|\nabla U_h^n\|_{L^2(\Omega_h^n)} \\
(27)\qquad & + \|\nabla(U_h^n - \bar{U}_h^{n-1})\|_{L^2(\Omega_h^n)}\Big] \|\nabla v\|_{L^2(\Omega(t))}.
\end{aligned}
$$

Similarly, we can estimate the term III

$$\begin{aligned} \mathrm{III} &= \int_{\hat\Omega} \hat D F_{t^n}^{-T}\hat\nabla \hat U_h^n \cdot \hat D F_{t^n}^{-T}\hat\nabla\hat v J_n d\hat x - \int_{\hat\Omega} \hat D F_t^{-T}\hat\nabla \hat U_h^n\cdot \hat D F_t^{-1}\hat\nabla \hat v J d\hat x \\ &\le C\tau_n \|\hat\nabla \hat U_h^n\|_{L^2(\hat\Omega)}\|\hat\nabla \hat v\|_{L^2(\hat\Omega)} \\ &\le C\tau_n\|\nabla U_h^n\|_{L^2(\Omega_h^n)}\|\nabla v\|_{L^2(\Omega(t))}. \end{aligned} \tag{28}$$

To estimate II, we first let $\Pi_h^n : L^1(\Omega_h^n) \to \overset{\circ}{V}{}_h^n(\Omega_h^n)$ be the modified Clément interpolation operator defined in (7) over the mesh $\mathcal{M}^n$. By (14) and (26) we know that

$$(\partial_t U_h(\cdot,t^n), \Pi_h^n V_n)_{\Omega_h^n} + (\nabla U_h^n, \nabla \Pi_h^n V_n)_{\Omega_h^n} = (f^n, \Pi_h^n V_n)_{\Omega_h^n}.$$

Now since $V_n \in H_0^1(\Omega^n)$ and $\Omega^n \subset \Omega_h^n$, we have then

$$\begin{aligned} \mathrm{II} &= (f^n - \partial_t U_h(\cdot,t^n), V_n - \Pi_h^n V_n)_{\Omega_h^n} - (\nabla U_h^n, \nabla(V_n - \Pi_h^n V_n))_{\Omega_h^n} \\ &= (R^n, V_n - \Pi_h^n V_n)_{\Omega_h^n} - (\nabla U_h^n, \nabla(V_n - \Pi_h^n V_n))_{\Omega_h^n}. \end{aligned}$$

Now the argument in the proof of Theorem 2.5 yields

$$\begin{aligned} \mathrm{II} &\le C\left(\|U_h^n\|^2_{H^{1/2}(\Gamma^n)} + \sum_{K\in\mathcal{M}^n}\eta^2_{K,n}\right)^{1/2}\|\nabla V_n\|_{L^2(\Omega^n)} \\ &\le C\left(\|U_h^n\|^2_{H^{1/2}(\Gamma^n)} + \sum_{K\in\mathcal{M}^n}\eta^2_{K,n}\right)^{1/2}\|\nabla v\|_{L^2(\Omega(t))}. \end{aligned} \tag{29}$$

Collecting the estimates (21)-(25), (27)-(29), and (19) we have

$$\begin{aligned} &\int_0^T \|f_1\|^2_{H^{-1}(\Omega(t))}dt \\ \le\ & C\sum_{n=1}^N \tau_n \sum_{K\in\mathcal{M}^n}\left(\eta^2_{K,n} + h_K\|\nabla U_h^n\|^2_{L^2(K\cap\Gamma^n)}\right) + C\sum_{n=1}^N\int_{t^{n-1}}^{t^n}\|f-\tilde f^n\|^2_{L^2(\Omega(t))}dt \\ +\ & \sum_{n=1}^N \tau_n\left[\tau_n^2\|R^n\|^2_{L^2(\Omega_h^n)} + \tau_n^2\|\nabla U_h^n\|^2_{L^2(\Omega_h^n)} + \|\nabla(U_h^n - \bar U_h^{n-1})\|^2_{L^2(\Omega_h^n)}\right]. \end{aligned}$$

This competes the proof after using Lemma 4.3. □

5. The adaptive algorithm and numerical examples

The implementation of our algorithms is based on the adaptive finite element package ALBERTA [31]. We first consider the adaptive immersed finite element method for elliptic problems in section 5.1 and then for parabolic problems in section 5.2.

5.1. Elliptic Problem. For the elliptic problem we start with an initial mesh over a polygonal domain that contains Ω. This initial mesh is adaptively refined and we require that through the adaptive refinement procedures, the boundary of the domain Γ intersects the sides of each element of the mesh at most twice as required by the definition of our immersed finite element method. We will consider only homogeneous boundary condition $g = 0$. By Theorem 2.5 and Corollary 2.8 we use the following local a posteriori error estimator

$$\eta_K^2 = h_K^2\|f\|^2_{L^2(K)} + \sum_{e\in\mathcal{E}(K)} h_K\|[\![\nabla u_h\cdot\mathbf{n}]\!]_e\|^2_{L^2(e)} + h_K\|\nabla u_h\|^2_{L^2(K\cap\Gamma)}.$$

The set of the elements marked for refinement $\hat{\mathcal{M}}_h$ is determined by the following Dörfler strategy [13].

$$\left(\sum_{K\in\hat{\mathcal{M}}_h}\eta_K^2\right)^{1/2}\geq\frac{1}{2}\left(\sum_{K\in\mathcal{M}_h}\eta_K^2\right)^{1/2}.$$

EXAMPLE 1. We consider a problem whose exact solution is known to illustrate the effectiveness index of the a posteriori error estimate. We solve $-\Delta u=f$ in Ω with zero boundary condition, where

$$\Omega=\left\{x\in\mathbb{R}^2:\ (2x_1)^2+\left(\frac{3x_2}{10}\right)^2>1\ \text{ and } x_1^2+x_2^2<1\right\}.$$

The exact solution is

$$u=(1-x_1^2-x_2^2)\left((2x_1)^2+\left(\frac{3x_2}{10}\right)^2-1\right).$$

The effectiveness index **eff** of the a posteriori error estimate is defined by $\mathbf{eff}=\eta/\mathscr{E}$, where $\eta=\left(\sum_{K\in\mathcal{M}_h}\eta_K^2\right)^{1/2}$ and $\mathscr{E}=||\nabla(u-u_h)||_\Omega$. In Table 5.1 we report the number of nodes $N,\eta,\mathscr{E}$, and **eff** for different choices of `TOL`. The adaptive algorithm terminates whenever $\eta\leq$ `TOL` is satisfied. We observe that the error $\mathscr{E}$ is reduced by half when the number of degrees of freedom is increased roughly four times. The effectiveness index **eff** remains roughly constant when `TOL` is reduced.

TABLE 1. The number result of different values of TOL_{space}.

`TOL`	N	η	$\mathscr{E}$	**eff**
$\sqrt{2}$	10528	1.315	0.1570	8.3771
$\sqrt{0.5}$	41353	0.662	0.0805	8.2150
$\sqrt{0.125}$	154723	0.3402	0.04141	8.2161

EXAMPLE 2. We consider in this example a problem with a singular solution to illustrate the competitive behavior of our adaptive algorithm. Let the domain Ω have a reentrant corner with curved boundary as illustrated in Fig. 5. We consider the equation $-\Delta u=1$ in Ω with the boundary condition $g=0$.

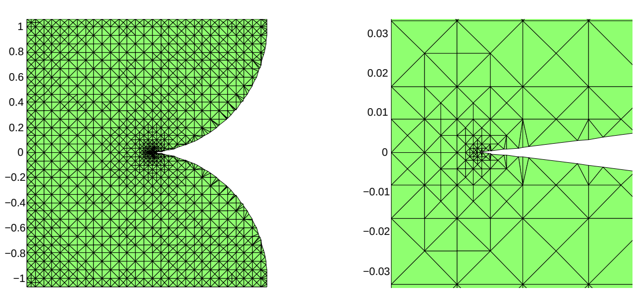

FIGURE 5. The mesh of 2898 elements after 16 adaptive refinement steps (left) and a part of the zoomed mesh (right).

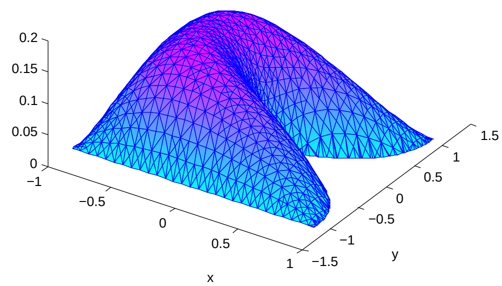

FIGURE 6. The discrete solution on the mesh of 2898 elements.

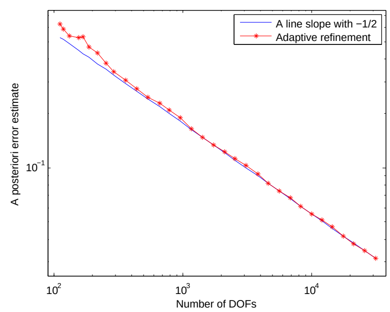

FIGURE 7. Quasi-optimality of the adaptive mesh refinements of the a posteriori error estimates.

Fig. 5 shows an adaptively refined mesh of 2898 elements and a part of the zoomed mesh. The solution on this mesh is shown in Fig. 6. We observe that the mesh is much refined around the tip of corner where the solution is singular. Fig. 7 shows the plot of $\log N - \log \eta$, where N is the number of degrees of freedom and $\eta = \left(\sum_{K \in \mathcal{M}_h} \eta_K^2\right)^{1/2}$ is the total estimated error. It indicates clearly that the meshes and the associated numerical compexity are quasi-optimal: $\eta \approx CN^{-1/2}$ is valid asymptotically.

5.2. Parabolic problem. Now we turn to the adaptive algorithm for parabolic problems in the time variable domain. We first describe how to construct the ALE mapping $F_{n-1}^n := F_{t^{n-1}} \circ F_{t^n}^{-1}$ used in calculation of the pullback $\bar{U}_h^{n-1}$ in (3.4). At n-th time step, we assume the new position of the boundary is given by a boundary mapping $\mathrm{g} : \partial\Omega^n \to \partial\Omega^{n-1}$. The mapping F_{n-1}^n is defined by solving the Laplace equation:

$$-\Delta F_{n-1}^n = 0 \text{ in } \Omega^n, \qquad F_{n-1}^n = \mathrm{g} \text{ on } \partial\Omega^n \tag{30}$$

The immersed finite element method in section 2 is used to discretize this problem in Ω_h^n.

To compute $\bar{U}^{n-1} = U^{n-1}(F_{n-1}^n(x))$ once we have F_{n-1}^n at hand, we have to do Lagrange interpolation in an efficient way. The central issue is, for any $x \in K_0 \subset \mathcal{M}^n$, we need to locate the simplex $K' \in \mathcal{M}^{n-1}$ which includes $x' = F_{n-1}^n(x)$.

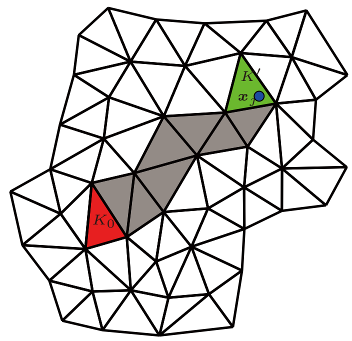

FIGURE 8. Locate the element $K' \in \mathcal{M}^{n-1}$ which includes $x' = F_{n-1}^n(x)$.

Our implementation first looks for the macro-element containing x' and then finds its path through the corresponding element tree based on the macro barycentric coordinates. In ALBERTA [31], which works on hierarchical triangulations, we can perform this operation locally on every mesh element and find the leaf element K' containing this x' in an optimal way. For points x close to the boundary it may happen that x' does not belong to the computational domain. In this case, we set $\bar{U}_h^{n-1}(x) = 0$ as described in section 3.

To begin with the time and space adaptation, we first obtain an initial mesh $\mathcal{M}^0$ over a polygonal domain Ω_h^0 that contains $\Omega(0)$ and controls the initial error $\|u_0 - U_h^0\|_{L^2(\Omega(0))}$, where U_h^0 is the approximation of the initial condition which is usually taken as the Lagrange interpolation of u_0 for smooth u_0. Other approximation is also possible if u_0 has lower regularity.

For $n \geq 1$, we define the total time error indicator $\eta_{\rm time}^n$ and the space error indicator $\eta_{\rm space}^n$ by

$$\begin{aligned}
\eta_{\rm time}^n &= \Big(\tau_n^2\|R^n\|_{L^2(\Omega_h^n)}^2 + \tau_n^2\|\nabla U_h^n\|_{L^2(\Omega_h^n)}^2 + \|\nabla(U_h^n - \bar{U}_h^{n-1})\|_{L^2(\Omega_h^n)}^2 \\
&\quad + \|(U_h^n - \bar{U}_h^{n-1})/\tau_n\|_{L^2(\Gamma^n)}^2\Big)^{1/2}, \\
\eta_{\rm space}^n &= \left(\sum_{K\in\mathcal{M}^n} \tilde{\eta}_{K,n}^2\right)^{1/2}, \qquad \tilde{\eta}_{K,n}^2 = \eta_{K,n}^2 + h_K\|\nabla U_h^n\|_{L^2(K\cap\Gamma^n)}^2,
\end{aligned}$$

where the local error indicator $\eta_{K,n}$ is defined in Theorem 4.4. The proposed adaptive algorithm can be summarized as follows:

Algorithm 5.1. Given tolerances $\texttt{TOL}_{\texttt{time}}$ and $\texttt{TOL}_{\texttt{space}}$. Given the initial mesh $\mathcal{M}^0$ and U_h^0, τ_0. Set $n = 1$, $t_0 = 0$.

• Time iteration: Let U_h^{n-1} be computed from the previous time step at time t^{n-1} with the mesh $\mathcal{M}^{n-1}$ and time step size τ_{n-1}. Do while $t < T$

- $\mathcal{M}^n := \mathcal{M}^{n-1}, \tau_n := \tau_{n-1}, t := t_n = t + \tau_n$;
- Construct mapping $F_{n-1}^n := F_{t^{n-1}} \circ F_{t^n}^{-1}$ according to (30);
- Use F_{n-1}^n to calculate $\bar{U}_h^{n-1}$;
- Solve U_h^n according to (3.5);
- Compute the time error estimator $\eta_{\rm time}^n$ and the local error indicator $\tilde{\eta}_{K,n}$, summing them up to get $\eta_{\rm space}^n$;
- Perform mesh and time-step adaptation:

- ◦ If η^n_{time} is too small or too large, $t := t - \tau_n$, adjust time step until time threshold is reached

$$(\eta^n_{\text{time}})^2 + \int_{t^{n-1}}^{t^n} \|f - \tilde{f}^n\|^2_{L^2(\Omega(t))} dt \leq \frac{\texttt{TOL}_{\texttt{time}}{}^2}{T},$$

- ◦ If $(\eta^n_{\text{space}})^2 > \texttt{TOL}_{\texttt{space}}{}^2/T$, mark the set of elements for refinements $\mathcal{M}^n_{\text{refine}}$ or for coarsening $\mathcal{M}^n_{\text{coarse}}$ according to the Dörfler strategy [14]:

$$\sum_{K \in \mathcal{M}^n_{\text{refine}}} \tilde{\eta}^2_{K,n} \geq \theta_r^2 \sum_{K \in \mathcal{M}^n} \tilde{\eta}^2_{K,n}, \qquad \sum_{K \in \mathcal{M}^n_{\text{coarse}}} \tilde{\eta}^2_{K,n} \leq \theta_c^2 \sum_{K \in \mathcal{M}^n} \tilde{\eta}^2_{K,n}.$$

  Terminate the iteration for the mesh adaptation whenever $(\eta^n_{\text{space}})^2 \leq \texttt{TOL}_{\texttt{space}}{}^2/T$ is satisfied.

- Set $n := n + 1$.

We refer to the Algorithm 3.2 of [7] for further implementation details. We define η_{total} the total estimated error

$$\eta^2_{\text{total}} = \sum_{n=1}^{N} \tau_n \left[(\eta^n_{\text{space}})^2 + (\eta^n_{time})^2 \right].$$

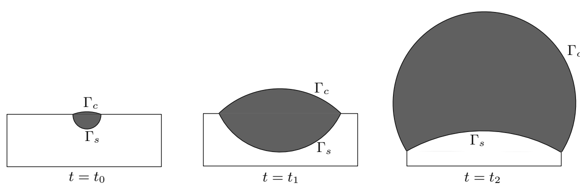

Figure 9. Geometric setting of Example 3.

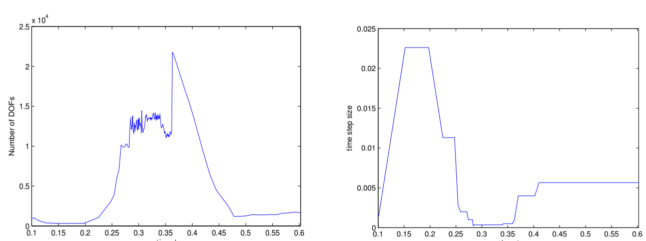

Figure 10. The number of nodes and time step sizes at each time step n (Example 3).

Example 3. The first example is motivated from [5] which studies the temperature driven melting of a thin wire end. Fig. 9 shows a sequence of geometric settings, where $\Gamma(t) = \Gamma_C(t) \cup \Gamma_S(t)$, denoting the free capillary surface and the phase transition front, respectively. Here we only consider the problem (1.1)-(1.3)

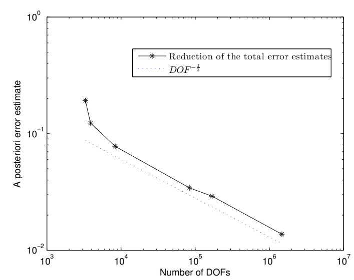

FIGURE 11. Quasi-optimality of the adaptive algorithm for Example 3.

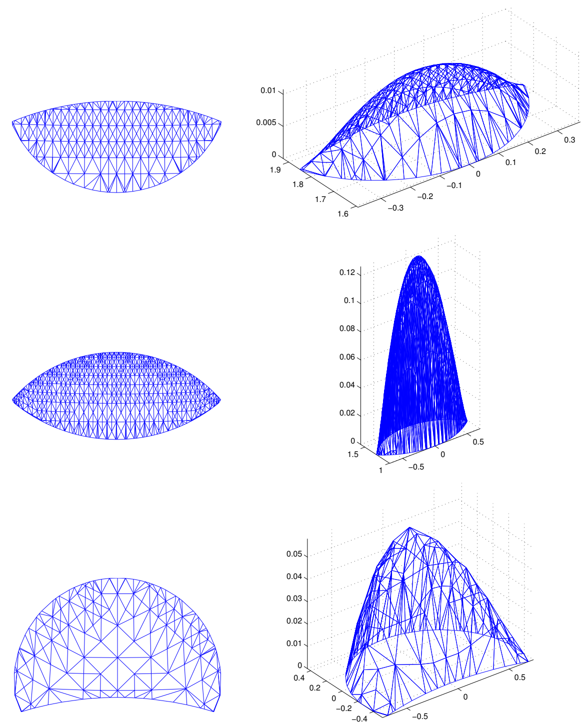

FIGURE 12. The solutions and corresponding adaptive meshes at time $t = 0.12490, 0.27471, 0.59694$ (from top to bottom). The numbers of nodes of the meshes are 279, 488, 124, respectively (Example 3).

in the melting region $\Omega(t)$ (shadow region in FIG. 9) and prescribe the moving boundary $\Gamma_C(t), \Gamma_S(t)$ as follows

$$\Gamma_C(t) = \{(x_1, x_2) \in \mathbb{R}^2 |\ x_1 = r_C \sin\phi, x_2 = r_C \cos\phi + \cos\theta, \phi \in (-\theta, \theta)\},$$
$$\Gamma_S(t) = \Big\{(x_1, x_2) \in \mathbb{R}^2 |\ x_1 = -r_S \sin\phi, x_2 = -r_S \cos\phi + \frac{r_C}{\cos\theta} + \cos\theta,$$
$$\phi \in \Big(-\Big|\theta - \frac{\pi}{2}\Big|, \Big|\theta - \frac{\pi}{2}\Big|\Big)\Big\},$$

where $r_C = \min\left(1, \frac{1}{\sqrt{2}\sin\theta}\right)$, $r_S = r_C \tan\theta$ with $\theta = \pi(t + 0.1)$.

The initial condition is $u_0 = 0$. We introduce a time singularity through the source

$$f(t) = \begin{cases} 1.0, & \text{if } t \le 0.2, t > 0.4, \\ 5 - 40|t - 0.3|, & \text{if } 0.2 < t \le 0.4. \end{cases}$$

Let $M = \sum_{n=1}^{N} M_n$ be the total number of nodes, where M_n is the number of nodes at time t^n. FIG. 11 shows the plot of $\log M$-$\log \eta_{\text{total}}$ which indicates that our adaptive algorithm has the very desirable quasi-optimal computational complexity: $\eta_{total} \approx CM^{-1/3}$.

FIG. 12 shows the meshes and the surface plots of the solutions at various time steps when $\texttt{TOL}_{\texttt{time}} = \texttt{TOL}_{\texttt{space}} = 0.02$. The number of nodes and time step size at each time step n are shown in FIG. 10. We observe that the time step size is fairly large at the starting stage and drops around a small time interval $[0.2, 0.4]$ while remains almost constant afterwards. That is not surprising since the temperal domains are relatively small at the beginning of the simulation and $f(t)$ changes from 1 to 5 and then from 5 to 1 around $t = 0.3$.

EXAMPLE 4. We consider a rigid valve model in this example (see [16]). The domain is depicted in Fig 13, where there is an inner boundary $\Gamma_1(t)$(valve) moving periodically in t with $\theta(t) = \frac{\pi t}{6}$. On the top boundary Γ_2, we impose a natural boundary condition $\frac{\partial u}{\partial \mathrm{n}} = (0.5625 - x^2) \cdot t$, which reflects the inflow or outflow of the flux. On the other part of the boundary, we set $u = 0$. Let the source $f = 0$.

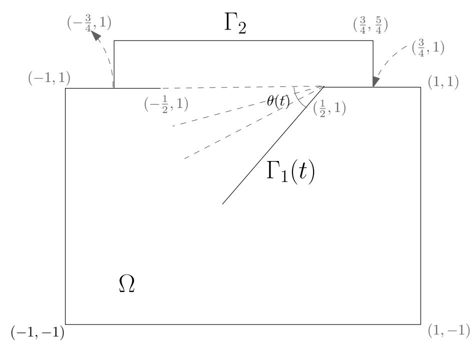

FIGURE 13. Geometric setting of Example 4.

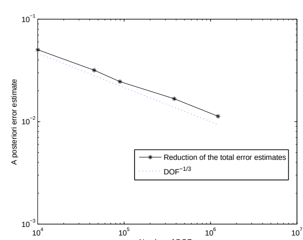

FIGURE 14. Quasi-optimality of the adaptive algorithm for Example 4.

FIG. 14 shows the $\log M$-$\log \eta_{\text{total}}$ curves, where η_{total} is the total error estimates and M is the total number of degrees of freedom. It indicates that the adaptive meshes and the associated computational complexity are quasi-optimal: $\eta_{total} \approx$

$CM^{-1/3}$ is valid asymptotically. The meshes and surface plots of corresponding solutions at various time steps are displayed in Fig. 15. We note the mesh is locally refined around the tips and near the cusp points where the solution is singular.

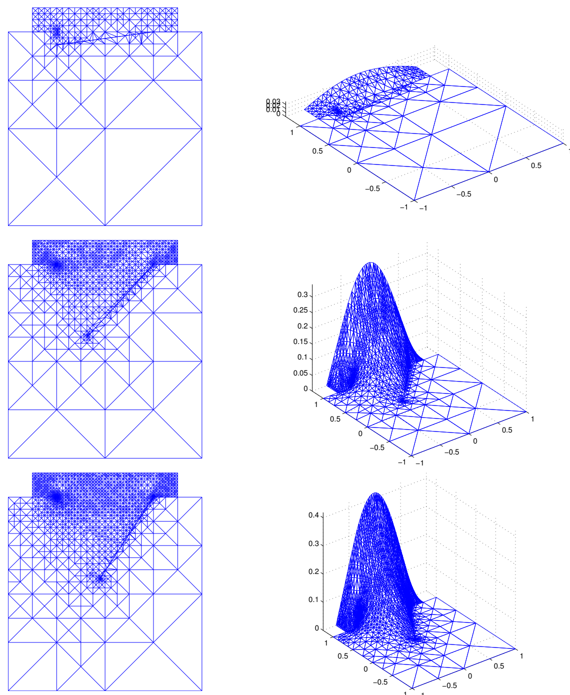

Figure 15. The solutions and corresponding adaptive meshes at time $t = 0.27009, 1.6630, 1.9830$ (from top to bottom). The numbers of nodes of the meshes are 302, 1319, 2001, respectively (Example 4).

References

[1] R. A. Adams and J. J. F. Fournier, Sobolev Spaces, 2nd Edition, Academic Press, Amsterdam, 2003.

[2] G. Allaire and A. Henrot, On some recent advances in shape optimization, C.R. Acad. Sci. Paris, Ser. II b, 329 (2001) 383-396.

[3] I. Babuska and A.K. Aziz, On the angle condition in the finite element method, SIAM J. Numer. Anal., 13 (1976) 214–226.

[4] S. Badia, A. Quaini, and A. Quarteroni, Splitting methods based on algebraic factorization for fluid-structure interaction, SIAM J. Sci. Comput., 30 (2008) 1778–1805.

[5] E. Bäsch, J. Paul, and A. Schmidt, An ALE finite element method for a coupled Stefan problem and Navier-Stokes equations with free capillary surface, Int. J. Numer. Meth. Fluids, 71 (2013) 1282–1296.

[6] Z. Chen and G. Ji, Sharp L^1 a posteriori error analysis for nonlinear convection-diffusion problems, Math. Comp., 75 (2006) 43-71.

[7] Z. Chen and J. Feng, An adaptive finite element method with reliable and efficient error control for linear parabolic problems, Math. Comp., 73 (2004) 1163–1197.

[8] Z. Chen, Y. Xiao, and L. Zhang, The adaptive immersed interface finite element method for elliptic and Maxwell interface problems, J. Comput. Phys., 228 (2009) 5000–5019.

[9] Z. Chen and H. Wu, Selected Topics in Finite Element Methods, Science Press, Beijing, 2010.

[10] C. C. Chu, I.G. Graham, and T. Y. Hou, A new multiscale Finite Element method for high-contrast elliptic interface problems, Math. Comp., 79 (2010) 1915-1955.

[11] P. Clément, Approximation by finite element functions using local regularization, RAIRO Anal. Numer., 9 (1975) 77–84.
[12] W. Dörfler and M. Rumpf, An adaptive strategy for elliptic problems including a posteriori controlled boundary approximation, Math. Comp., 67 (1998) 1361-1382.
[13] W. Dörfler, A convergent adaptive algorithm for Possion's equations, SIAM J. Numer. Anal., 33 (1996) 1106-1124.
[14] W. Dörfler, A time and space adaptive algorithm for the linear time-dependent Schrödinger equation, Numer. Math., 73 (1996) 419-448.
[15] B. Faermann, Local a-posteriori error indicators for the Galerkin discretrization of boundary integral equations, Numer. Math., 79 (1998) 43-76.
[16] L. Formaggia, A. Quarteroni, and A. Veneziani (Eds.), Cardiovascular Mathematics, Springer-Verlag Italia, Milano, 2009.
[17] G. P. Galdi and R. Rannacher (Eds.), Fundamental Trends in Fluid-Structure Interaction, World Scientific, Singapore, 2009.
[18] L. Gerardo-Giorda, F. Nobile, and C. Vergara, Analysis and optimization of Robin-Robin partitioned procedures in fluid-structure interaction problems, SIAM J. Numer. Anal., 48 (2010) 2091-2116.
[19] P. Jamet, Estimations d'erreur pour des éléments finis droits presque dégénérés, RAIRO Anal. Numer., 10 (1976) 43-61.
[20] P. Jamet, Galerkin-type approximations which are discontinuous in time for parabolic equations in a variable domain, SIAM J. Numer. Anal., 5 (1978) 912–928.
[21] C.E. Kenig, Harmonic Analysis Techniques for Second Order Elliptic Boundary Value Problems, CBMS Regional Conference Series in Mathematics, Number 83, American Mathematical Society, 1994.
[22] R. LeVeque and Z. Li, The immersed interface method for elliptic equations with discontinuous coefficients and singular sources, SIAM J. Numer. Anal., 31 (1994) 1019–1044.
[23] J. Li, J. M. Melenk, B. Wohlmuth, and J. Zou, Optimal a priori estimates for higher order finite elements for elliptic interface problems, Appl. Numer. Math., 60 (2010) 19–37.
[24] Z. Li and K. Ito, The immersed interface method: numerical solutions of PDEs involving interfaces and irregular domains, SIAM, Philadephia, 2006.
[25] Z. Li, T. Lin, and X. Wu, New Cartesian grid methods for interface problems using the finite element formulation, Numer. Math., 96 (2003) 61–98.
[26] G. P. Liang and Z. Chen, A full-discretization moving FEM with optimal convergence rate, Chinese J. Num. Math. & Appl., 12 (1990) 91-111.
[27] X. Liu, R. P. Fedkiw, and M. Kang, A boundary condition capturing method for Poissons equation on irregular domains, J. Comput. Phys., 160 (2000) 151–178.
[28] C. S. Peskin, Numerical analysis of blood flow in heart, J. Comput. Phys., 25 (1977) 220–252.
[29] M. Picasso, Adaptive finite elements for a linear parabolic problem, Comput. Methods Appl. Mech. Engrg., 167 (1998) 223-237.
[30] R. Sacchi and A. Veeser, Locally efficient and reliable a posteriori estimators for Dirichlet problems, Math. Model. Meth. Appl. Sci., 16 (2006) 319-346.
[31] A. Schmidt, K. G. Siebert, Design of Adaptive Finite Element Software: The Finite Element Toolbox ALBERTA. Springer, 2005.
[32] G. C. Verchota, Layer potentials and boundary value problems for Laplace's equation in Lipschitz domain, J. Funct. Anal., 59 (1984) 572-611.

LSEC, Institute of Computational Mathematics, Academy of Mathematics and System Sciences, Chinese Academy of Sciences, Beijing 100190, People's Republic of China
E-mail: zmchen@lsec.cc.ac.cn
URL: http://lsec.cc.ac.cn/∼zmchen/

Institute of Computational Mathematics, Academy of Mathematics and System Sciences, Chinese Academy of Sciences, Beijing 100190, People's Republic of China
E-mail: wuzedong@lsec.cc.ac.cn

Department of Mathematics, Nanjing University, Nanjing 210093, People's Republic of China.
E-mail: xym@nju.edu.cn